Available online at www.sciencedirect.com
SCIENCE DIRECT®

Journal of the European Ceramic Society 23 (2003) 1599–1607
www.elsevier.com/locate/jeurceramsoc

Glass-ceramics containing ferroelectric bismuth germanate (Bi_2GeO_5)

K. Pengpat, D. Holland*

Department of Physics, University of Warwick, Coventry CV4 7AL, UK

Received 10 March 2002; received in revised form 22 October 2002; accepted 28 October 2002

Abstract

Glasses have been formed from the $BiO_{1.5}$–GeO_2–$BO_{1.5}$ system and a study made of their devitrification behaviour and the properties of the glass-ceramics obtained. Crystals of the ferroelectric phase, orthorhombic Bi_2GeO_5, are precipitated in all of the glass compositions studied and this is the dominant phase in the region of 60 mol% $BiO_{1.5}$:20 mol% GeO_2:20 mol% $BO_{1.5}$. The microstructures of the glass-ceramics have been found to change dramatically on altering the crystallisation temperature, yielding spherulites or surface crystallisation which can be used to produce oriented growth. The dielectric behaviour and ferroelectric hysteresis loop of a selected Bi_2GeO_5 glass-ceramic show that this material can be ferroelectric at room temperature with $P_s = 14\ \mu C/cm^2$.

Keywords: Bi_2GeO_5; Dielectric properties; Ferroelectric hysteresis loop; Glass-ceramics; Microstructure

1. Introduction

The Bi_2O_3-GeO_2 system produces some crystalline phases, such as $Bi_4(GeO_4)_3$ and $Bi_{12}GeO_{20}$, which possess valuable electrical properties. Nitsche[1] showed that large single crystals of bismuth germanate $Bi_4(GeO_4)_3$, with an electro-optic coefficient $r_{41} = 1.03 \times 10^{-10}$ cm/V, are easy to obtain by classical pulling techniques. $Bi_{12}GeO_{20}$, was also grown as a large single crystal. [2,3] The crystal structure is cubic with space group I23 and it has strongly piezoelectric properties with large electromechanical coupling constant and electro-optic effects. In the Bi_2O_3–GeO_2 system, four phases with stoichiometries 6:1, 1:1, 2:3 and 1:3 have been reported.[4,5] The phases 6:1 and 2:3, are thermodynamically stable. In the field of ferroelectric glass-ceramics, the Bi_2GeO_5 phase (1:1), having a high probability of being ferroelectric, is of particular interest.[6–8] Its composition contains 50 mol% GeO_2 and, since this is a good glass forming oxide, there is no need to add any further glass former as in the case of other ferroelectric glass-ceramics. Moreover, as this phase is metastable, and therefore difficult to produce by conventional ceramic methods, the glass-ceramic route provides a more feasible means of preparation. However, stoichiometric Bi_2GeO_5 cannot be prepared as the bulk precursor glass without some devitrification occurring, giving Bi_2GeO_5, $Bi_4(GeO_4)_3$ and β–Bi_2O_3 phases.[9,10] Nassau and Chadwick studied the glass forming region of Bi_2O_3–GeO_2 and found that bulk glasses could be obtained from compositions containing up to 50 mol% $BiO_{1.5}$.[10]

We report here the results of studies of glasses from the system $BiO_{1.5}$–GeO_2–$BO_{1.5}$, containing an additional glass former, B_2O_3, which permits a moderate melting temperature for the glass.

2. Experimental procedure

Glasses with selected compositions from the system $BiO_{1.5}$–GeO_2–$BO_{1.5}$ were produced by melting appropriate combinations of bismuth oxynitrate ($BiO\text{-}NO_3.H_2O$), germanium dioxide (GeO_2), and boric oxide (B_2O_3). Approximately 25 g of each composition were melted, in a 90Pt/10Rh crucible, in an air atmosphere, using an electric furnace. The melts were held at the melting temperatures (between 1000 and 1050 °C) for 15–30 mins. They were then splat-quenched between

* Corresponding author. Tel.: +44-2476-523-396; fax: +44-2476-692-016.
E-mail address: d.holland@warwick.ac.uk (D. Holland).

0955-2219/02/$ - see front matter © 2003 Elsevier Science Ltd. All rights reserved.
PII: S0955-2219(02)00410-7

liquid-nitrogen cooled copper plates or room temperature steel plates. Glass density was determined using a dedicated digital density balance with degassed, distilled water as the immersion fluid. Differential thermal analysis (DTA) was performed on finely powdered glass using a Stanton Redcroft DTA model 673-4 with heating rate of 10 °C min^{-1} and with quartz as the reference material. Crystallisation temperatures were identified from the DTA traces and the glasses were subjected to heat treatment schedules corresponding to each crystallisation temperature. The heating and cooling rates used were 5 °C min^{-1} and 10 °C min^{-1} respectively with 4 h dwell at temperature for complete crystallisation. X-ray diffraction was used to investigate the phase composition of the glass ceramics using a Philips powder diffractometer with CuK_α ($\lambda = 1.54178$ Å) radiation. The phases formed were identified by comparing the experimental diffraction patterns with the powder diffraction database.[11] A Jeol 6100 scanning electron microscope (SEM) was used to record backscattered electron images of the microstructure of the glass-ceramics and energy dispersive X-ray (EDX) analysis was used for compositional analysis of the bulk and of individual features. Thermal expansion was performed on a vertical silica dilatometer which was calibrated with a platinum standard. A heating rate of 2 °C min^{-1} was employed. Dielectric measurements of selected glass-ceramic samples were performed from room temperature up to 500 °C using an LCR meter over the frequency range 5Hz–13 MHz. The modified Sawyer–Tower circuit[12] with compensation added was used for ferroelectric loop measurement.[13] The samples were polished to 0.3 mm thickness and silver-paste electrodes of 2 mm diameter were applied on both sides of the samples. Input voltages in the range of 1–1.5 kV at 50–100 Hz were applied, the data were collected via a computer program and the hysteresis loops plotted.

Table 1
Nominal glass compositions in mol%

Sample	$BiO_{1.5}$ (mol%)	GeO_2 (mol%)	$BO_{1.5}$ (mol%)
$BiGe_S$ (S)	66.67	33.33	0
$BiGeB_1$ (1)	47.62	23.80	28.58
$BiGeB_2$ (2)	51.02	20.40	28.58
$BiGeB_3$ (3)	54.09	17.33	28.58
$BiGeB_4$ (4)	58.34	13.08	28.58
$BiGeB_5$ (5)	62.85	8.57	28.58
$BiGeB_6$ (6)	58.44	23.38	18.18
$BiGeB_7$ (7)	64.62	25.86	9.52

3. Results and discussion

3.1. Glasses

The compositions of the samples studied from the system $BiO_{1.5}$–GeO_2–$BO_{1.5}$ are shown in the ternary diagram in Fig. 1 and listed in Table 1. It should be noted that the formula units $BiO_{1.5}$ and $BO_{1.5}$ have been employed here so that polyhedral units can be directly equated with GeO_2.

The stoichiometric composition S (0% $BO_{1.5}$) partially devitrified on quenching. Sample $BiGeB_1$, which retained the stoichiometric ratio of Bi_2O_3 to GeO_2, was fully amorphous but produced only a minor amount of the Bi_2GeO_5 crystalline phase on heat treatment,

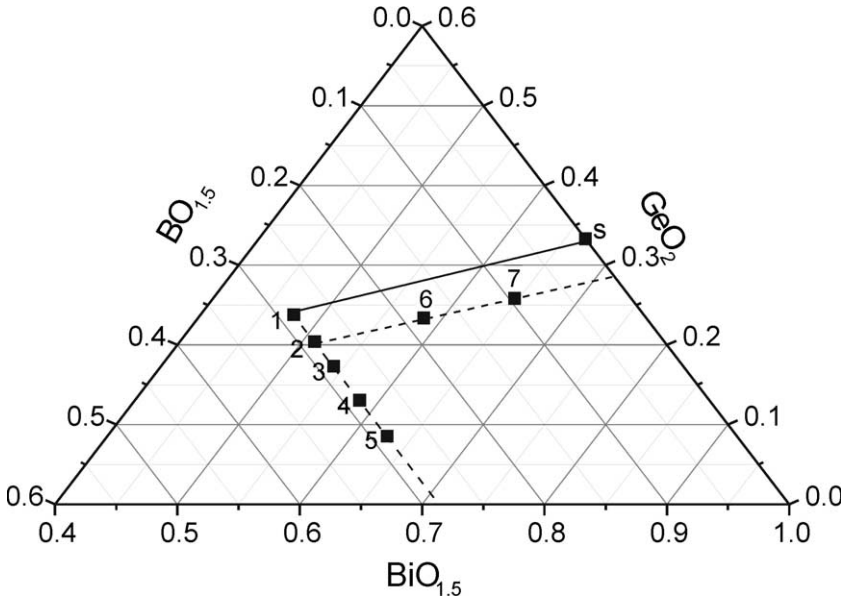

Fig. 1. The positions of the seven samples in the ternary diagram of the $BiO_{1.5}$–GeO_2–$BO_{1.5}$ system.

accompanied by $Bi_4(GeO_4)_3$. This indicates that some Bi^{3+} is retained in the borate residual glass phase and also that there may be compositional changes resulting from loss of volatile bismuth oxide (Bi_2O_3). Therefore, samples $BiGeB_2$ to $BiGeB_5$ were designed with excess Bi_2O_3 in order to compensate for these effects and to maximise the Bi_2GeO_5 phase content in the glass-ceramic. Samples $BiGeB_6$ and $BiGeB_7$ were also investigated to further maximise Bi_2GeO_5 phase content by reducing the boric oxide content. All compositions were amorphous within the detection limits of X-ray diffraction.

The variation of density of samples $BiGeB_1$ to $BiGeB_5$, with mol% $BiO_{1.5}$ and $BO_{1.5}$ is illustrated in Fig. 2. As would be expected, density increases with increasing $BiO_{1.5}$ content because of the substitution of Bi^{3+}, with its greater atomic mass, for Ge and decreases with addition of $BO_{1.5}$ which introduces extra network units with lower mass atoms. However, increase in density with $BiO_{1.5}$ content goes through a maximum as can be seen in Fig. 2a. This may indicate a change in the structural role of Bi^{3+} in the glass network. As will be shown in the next section, sample $BiGeB_4$ is the first sample to produce the bismuth borate phase ($BiBO_3$) on

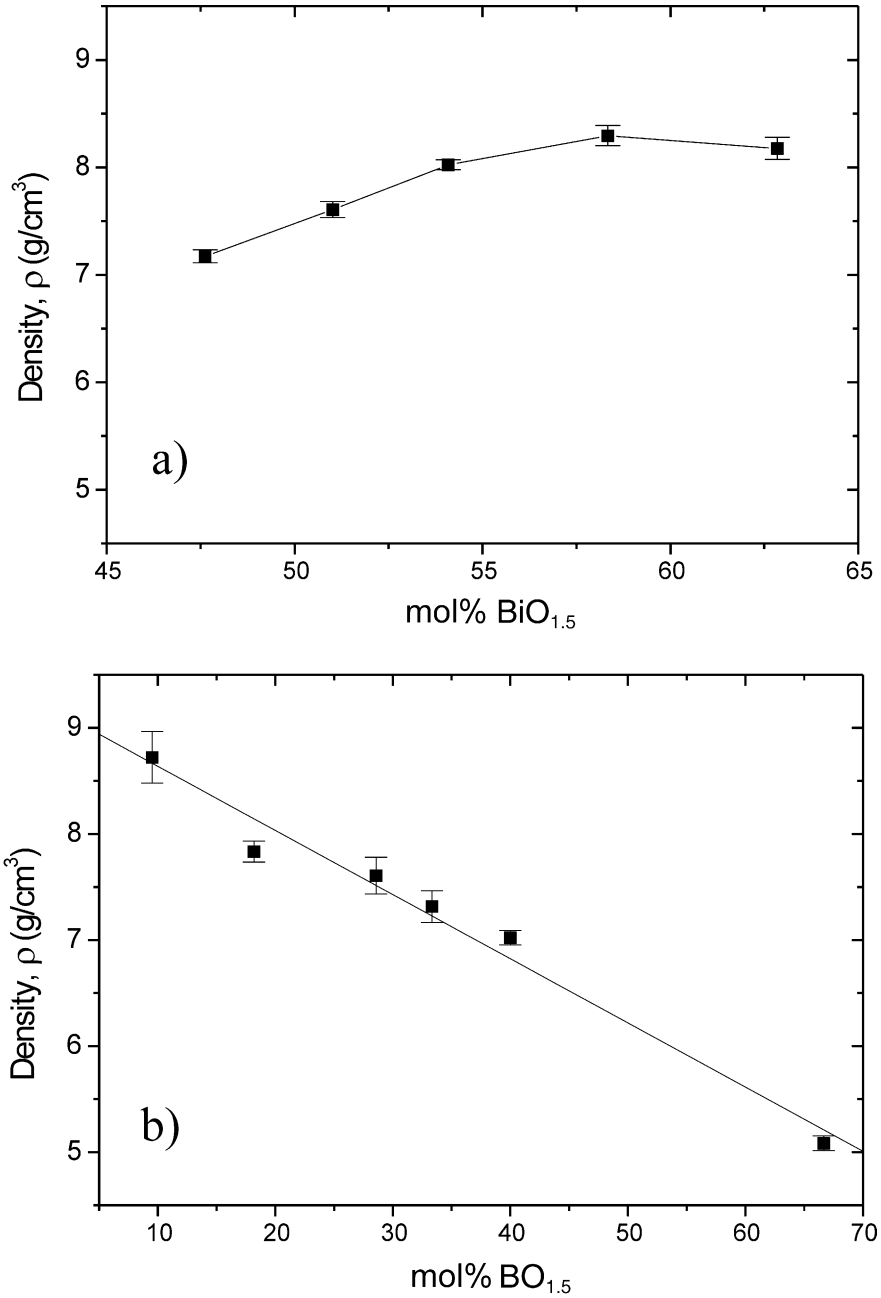

Fig. 2. (a) Density of $BiGeB_1$–$BiGeB_5$ samples (constant amount of 28.58 mol% $BO_{1.5}$) as a function of $BiO_{1.5}$ content. (b) Density as a function of $BO_{1.5}$ content for glasses with a $BiO_{1.5}$:GeO_2 ratio of 2.5:1.

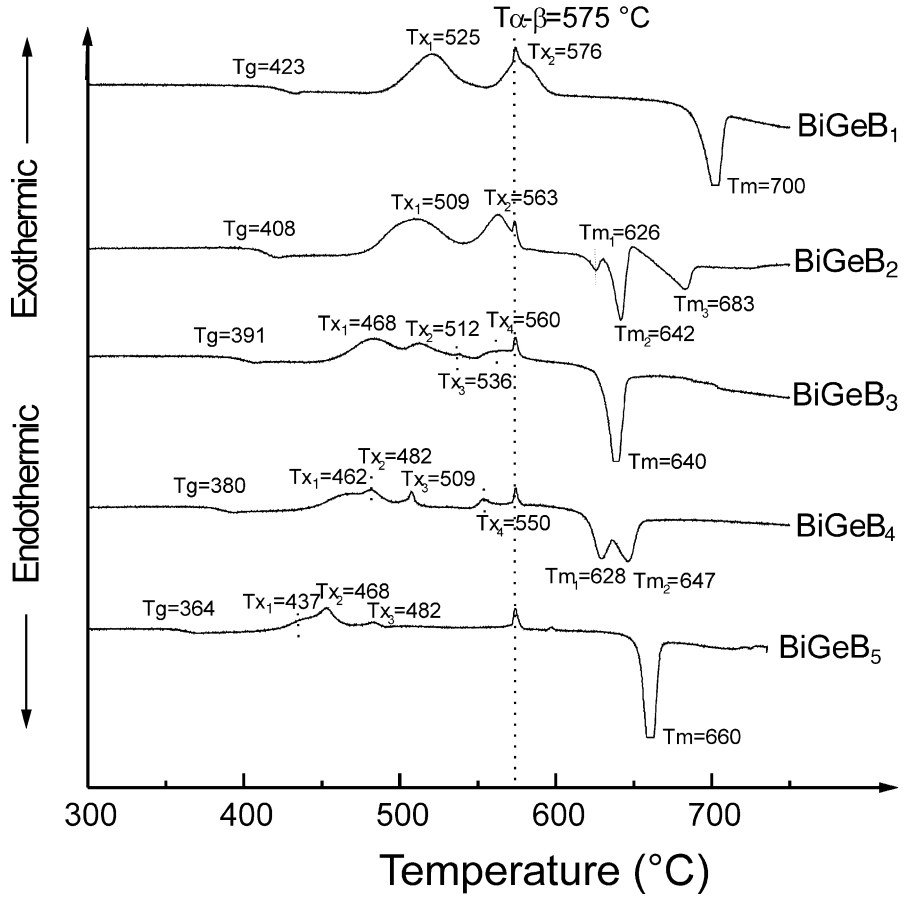

Fig. 3. DTA traces of samples $BiGeB_1$ to $BiGeB_5$.

crystallisation. This suggests that, at this point, the excess bismuth ion now acts as a modifier ion and, as the bismuth ions are larger than the interstices of isolated BO_3, they modify and increase the size of the interstices giving a decrease in glass density. From Fig. 2b, it can be seen that the relationship between the mol% of $BO_{1.5}$ and the density of the glasses is linear. This is similar to the binary systems, B_2O_3–GeO_2, where the density varies almost linearly with composition.[14]

3.2. Phase formation

The DTA traces of samples $BiGeB_1$ to $BiGeB_5$ are shown in Fig. 3 and are annotated with the glass transition temperatures (T_g), crystallisation temperatures (T_x) and melting points (T_m) which are then summarised in Table 2. The α–β quartz transition from the reference is indicated. Heat treatments at the various values of T_x were applied to the samples and the crystal phase information, obtained using X-ray diffraction, is also summarised in Table 2. It can be seen that Bi_2GeO_5 is the dominant phase over a wide composition range. SEM analysis was used to try to observe the unidentified phase in the $BiGeB_3$ sample. Fig. 4 illustrates the backscattered electron image from a cross-section

Table 2
Thermal parameters T_g (glass transition temperature), T_m (melting temperature) and T_x (crystallisation temperature) (the crystalline phases formed at each value of T_x are listed)

Sample	$T_g \pm 1$ (°C)	$T_m \pm 1$ (°C)	$T_x \pm 1$ (°C)	Crystalline phase[a]
$BiGeB_1$	423	700	525	$Bi_4(GeO_4)_3^{(I)}$, $Bi_2GeO_5^{(II)}$
			576	$Bi_4(GeO_4)_3^{(I)}$, $Bi_2GeO_5^{(II)}$
$BiGeB_2$	408	626, 642, 683	509	$Bi_4(GeO_4)_3^{(I)}$, $Bi_2GeO_5^{(II)}$
			563	$Bi_4(GeO_4)_3^{(I)}$, $Bi_2GeO_5^{(II)}$
$BiGeB_3$	391	640	468	$Bi_2GeO_5^{(II)}$ + unidentified phase
			512	$Bi_2GeO_5^{(II)}$ + unidentified phase
			536	$Bi_2GeO_5^{(II)}$ + unidentified phase
			560	$Bi_2GeO_5^{(II)}$ + unidentified phase
$BiGeB_4$	378	625, 645	462	$Bi_2GeO_5^{(II)}$, unidentified phase
			482	$Bi_2GeO_5^{(II)}$, $BiBO_3^{(III)}$
			509	$Bi_2GeO_5^{(II)}$, $BiBO_3^{(III)}$
			552	$Bi_2GeO_5^{(II)}$, $BiBO_3^{(III)}$
$BiGeB_5$	364	660	437	$Bi_2GeO_5^{(II)}$, $Bi_4B_2O_9$(IV), Bi_2O_3–$Bi_{24}GeO_{38}^{(V)}$
			468	$Bi_2GeO_5^{(II)}$, $Bi_4B_2O_9^{(IV)}$
			482	$Bi_2GeO_5^{(II)}$, $Bi_4B_2O_9^{(IV)}$
			598	$Bi_2GeO_5^{(II)}$, $Bi_4B_2O_9^{(IV)}$

[a] (I), (II), (III), (IV) and (V) refer to JCPDS 34-416, 36-289, 27-320, 25-1089 and 42–190 respectively. Some unlisted peaks at high angle were observed in every XRD pattern containing Bi_2GeO_5.

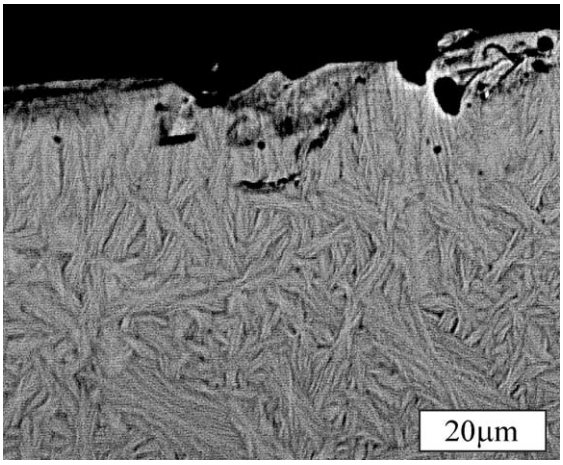

Fig. 4. SEM backscattered electron image of a cross-section through a $BiGeB_3$ glass-ceramic formed by heat treatment at 509 °C for 4 h.

through a $BiGeB_3$ sample heat treated at 468 °C. Spherulites of the Bi_2GeO_5 phase can be observed but no additional phase can be detected by differential contrast in the backscattered electron image and the unidentified phase cannot be discerned. Heat-treatment of $BiGeB_3$ at other crystallisation temperatures gave similar XRD patterns, containing Bi_2GeO_5 plus unidentified phase. Since this unidentified phase is observed at a low heat treatment temperature in $BiGeB_4$ but replaced by $BiBO_3$ at higher temperatures, it is possible that it corresponds to a metastable borate phase. After all the heat treatments, these glass-ceramics were easily fragmented, indicating low strength. This may be caused by the high porosity near the surface of the glass-ceramics as can be seen in the backscattered electron image (Fig. 4).

Samples $BiGeB_6$ and $BiGeB_7$, as shown in Fig. 1, were also investigated in an attempt to maximise the phase content of Bi_2GeO_5 by reducing the boric oxide content but without compromising glass stability. The ratio $BiO_{1.5}$:GeO_2 was kept equal to that of sample $BiGeB_2$ since this composition had shown the largest amount of Bi_2GeO_5. The XRD patterns of melt-quenched $BiGeB_6$ and $BiGeB_7$ are shown in Fig. 5. It can be seen that $BiGeB_7$ devitrified while cooling, giving rise to Bi_2GeO_5 crystals, but $BiGeB_6$ formed a good glass as confirmed by the amorphous XRD pattern. The devitrified $BiGeB_7$ sample disintegrated on cooling. The DTA trace of $BiGeB_6$ glass is illustrated in Fig. 6 and the phases formed on heat treatment at the different values of T_x for different times are summarised in Table 3. As a glass-ceramic is required to have high thermal shock resistance, the thermal expansion coefficient should be as low as possible to minimise strain from temperature gradients within materials. The linear thermal expansion coefficient (α_L) of $BiGeB_6$ glass in the 25–300 °C temperature range is about 8 MK^{-1} which is close to the values of 8.5–9 MK^{-1} reported by Topping et al.,[15] for bismuth germanate glasses containing 95–75 mol% GeO_2.

Fig. 7a and b show the SEM backscattered electron images of glass-ceramic $BiGeB_6$ heated at 467 and 475 °C for 4 h. Both glass-ceramics contain the Bi_2GeO_5 crystal phase. The glass-ceramics heated at 467 °C have spherulites as shown in Fig. 7a. However, by heating further to 475 °C, surface dendritic crystallisation occurred as shown in Fig. 7b, which is preferable in that it may enhance piezoelectric or pyroelectric properties. Fig. 8, shows the XRD pattern of ground powder and

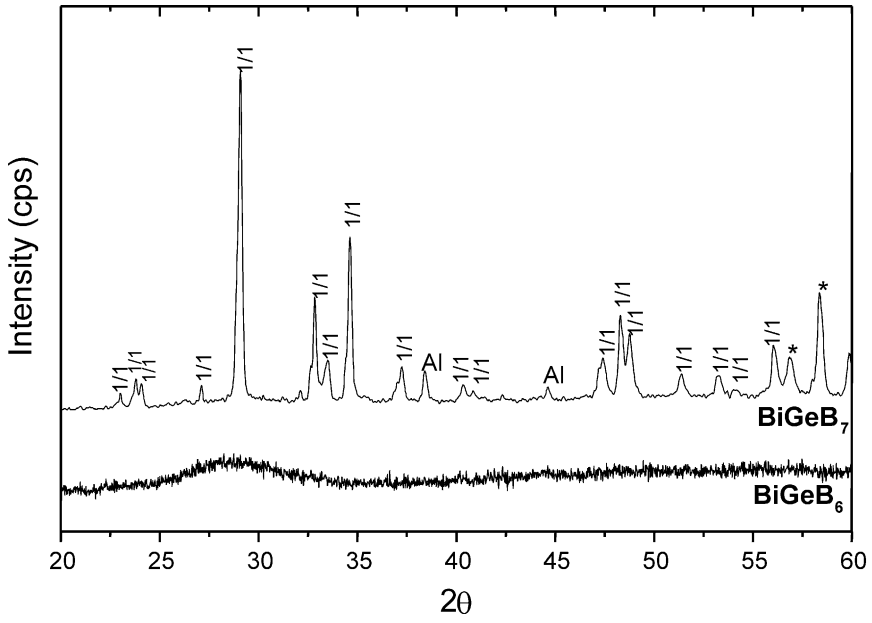

Fig. 5. XRD patterns of melt-quenched samples $BiGeB_6$ and $BiGeB_7$. Note: 1:1 = Bi_2GeO_5 (JCPDS No. 36-289) and * = unidentified peaks at high angle.

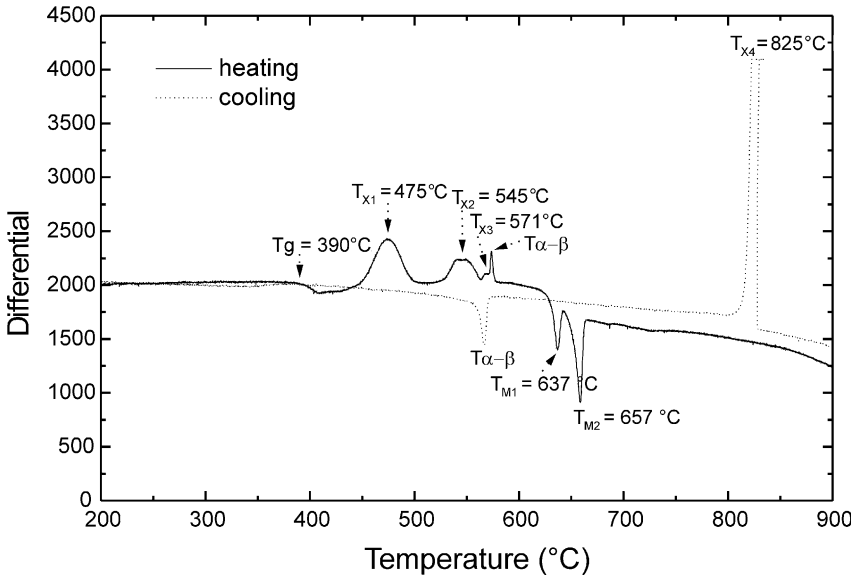

Fig. 6. DTA trace of $BiGeB_6$ glass.

also a bulk sample of $BiGeB_6$ subjected to heat treatment at 475 °C for 4 h. Preferred orientation in the bulk sample shows Bi_2GeO_5 growing perpendicular to (311) plane. The unidentified peak at $2\theta = 59.58$ may be identified as the (622) plane and this also corresponds to one of the unidentified peaks always observed in Bi_2GeO_5 containing samples. On this basis, the other unidentified peaks in the powder pattern can be associated with the 313 and 530 reflections (1.622 and 1.582 Å d-spacings respectively). These assignments are consistent with the reflection rules for the $Cmc2_1$ space group of Bi_2GeO_5.

3.3. Dielectric measurement

The $BiGeB_6$ glass-ceramic heat treated at 475 °C for 4 h showed no peak at the Curie temperature but, by increasing the dwell time to 12 h, the peak started to show at about 407 °C as seen in Fig. 9. This may be the result of the increase in mean crystallite size (determined from X-ray line broadening) from ~150 to ~200 nm on

Table 3
The crystal phases formed from different heat treatments of $BiGeB_6$ glass

Temperature (°C)	Dwell time (h)	Phase[a]
467	4	Bi_2GeO_5
$T_{X1} = 475$	0	Bi_2GeO_5
$T_{X1} = 475$	4	Bi_2GeO_5
$T_{X1} = 475$	12	Bi_2GeO_5
533	4	Bi_2GeO_5 + unidentified phase
$T_{X2} = 545$	4	Bi_2GeO_5 + unidentified phase
$T_{X3} = 571$	4	$Bi_2GeO_5 + Bi_4(GeO_4)_3$ + unidentified phase
$> T_{X4}$ and cool down	–	$Bi_4(GeO_4)_3$

[a] $Bi_4(GeO_4)_3$—JCPDS 34-416. Bi_2GeO_5—JCPDS 36-289. Some unlisted peaks at high angle were observed in every XRD pattern containing Bi_2GeO_5.

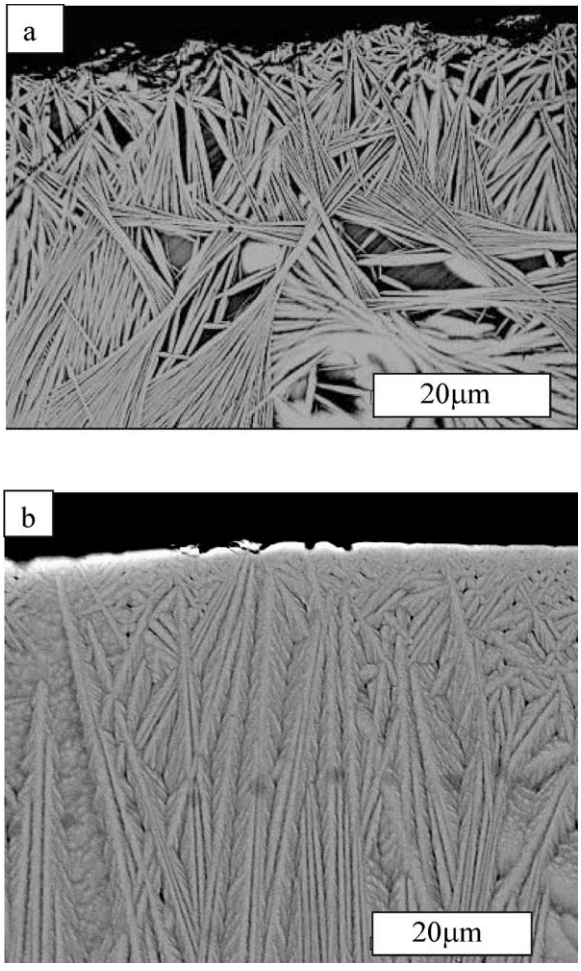

Fig. 7. (a) SEM backscattered electron image of a cross-section through a $BiGeB_6$ glass-ceramic heat treated at 467 °C for 4 h. (b) SEM backscattered electron image of a cross-section through a $BiGeB_6$ glass-ceramic heat treated at 475 °C for 4 h.

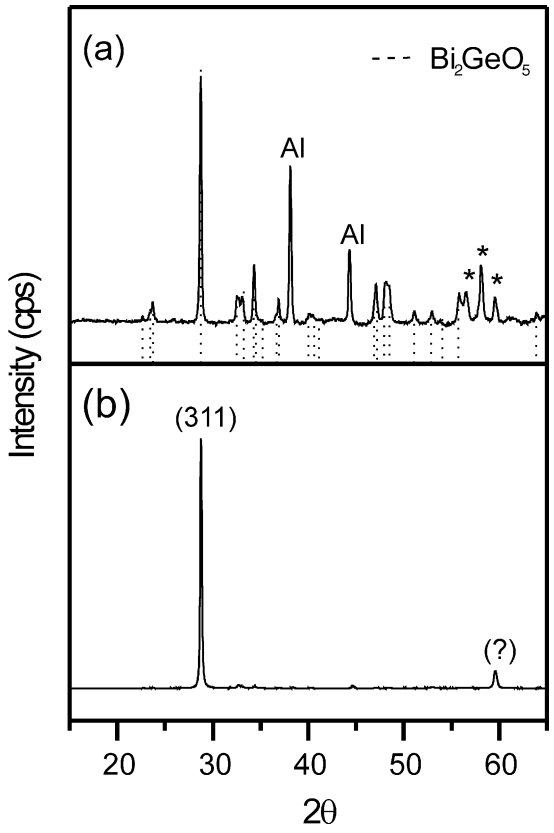

Fig. 8. XRD pattern of a $BiGeB_6$ glass-ceramic heat treated at 475 °C for 4 h: (a) powder and (b) bulk. Note: JCPDS No. of Bi_2GeO_5 is 36-289.

extending the heat treatment period from 4 h to 12 h. This is consistent with the report by Borelli and Layton,[16] that a cadmium-doped sodium niobate glass-ceramic showed a reduction in peak permittivity with decreasing crystallite size.

Fig. 10 shows the variation of the permittivities, K' and K'' with temperature, for different frequencies, of a $BiGeB_6$ glass-ceramic heat-treated at 475 °C for 12 h. It can be seen that the real part K' increases with increase in temperature at all frequencies from 10 kHz to 1 MHz. A peak in K' and K'' is observed around 407 °C. The peak in K' may be attributed to the phase-transition temperature of crystalline Bi_2GeO_5. Firsov et al.[6] suggested that single crystal Bi_2GeO_5 can be ferroelectric with $T_C > 800$ K (527 °C); therefore the shift in Curie temperature for the glass-ceramic must arise from the effects of the elastic and the electrostrictive forces exerted by the surrounding glass matrix on the crystallites contributing to the phase transition. Moreover, from the DTA cooling trace of $BiGeB_6$ glass (Fig. 6), the glass transition temperature is around 350 °C, so the Curie temperature of this glass-ceramic is well above the T_g of the residual glass phase whose high mobility, resulting in high elastic properties, may give rise to the shift in Curie temperature. This glass-ceramic has relatively low values of permittivity, typical of those normally found in many glass-ceramics, which does not make it suitable for the production of capacitors.

3.4. Hysteresis loop

A 240 μm thick sample of the Bi_2GeO_5 based glass-ceramic heat treated at 475 °C for 12 h, gave the ferroelectric hysteresis loop shown in Fig. 11, which has a value of remanent polarisation $P_s = 14.0 \pm 0.5$ μC/cm^2. A comparison of the ferroelectric properties of Bi_2GeO_5 with those of the important ferroelectric $BaTiO_3$ and related $Bi_4Ti_3O_{12}$ is made in Table 4. It can be seen that the P_s value of the Bi_2GeO_5 based glass-ceramic is

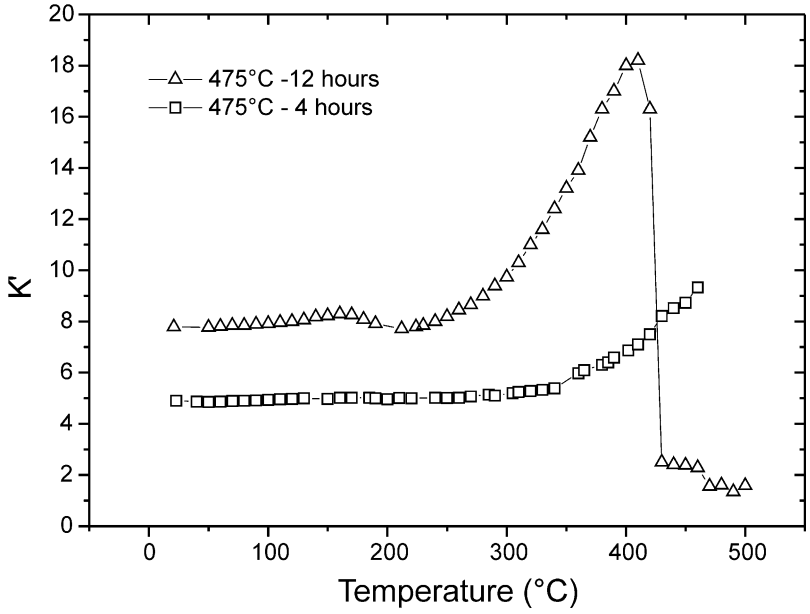

Fig. 9. Dielectric constant (at 10 kHz) versus temperature for $BiGeB_6$ glass-ceramics produced using different heat treatment schedules.

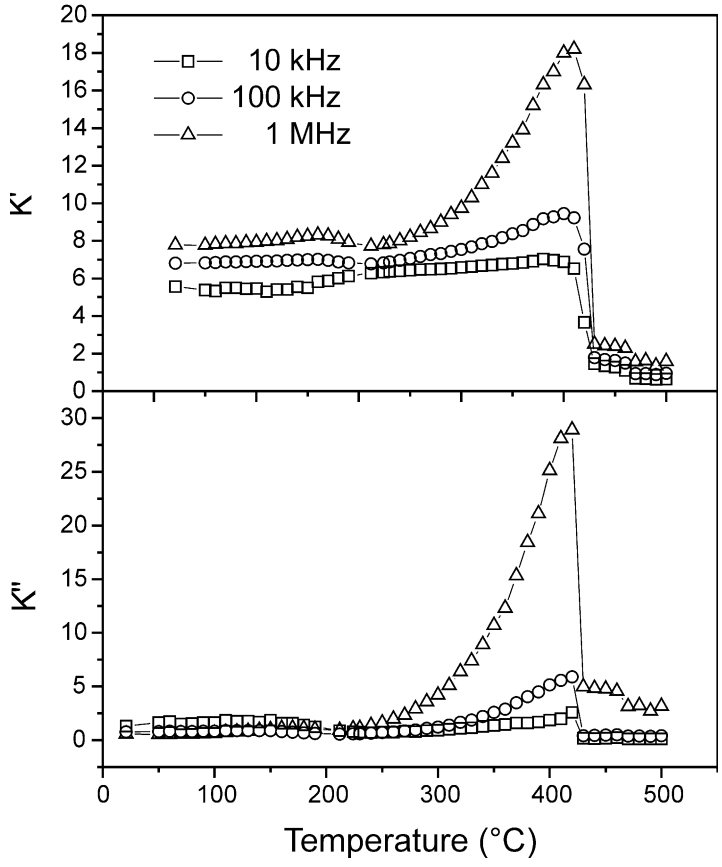

Fig. 10. Temperature dependence of real (K') and imaginary (K'') parts of the complex permittivity of a $BiGB_6$ thin sample (heat-treated at 475 °C for 12 h).

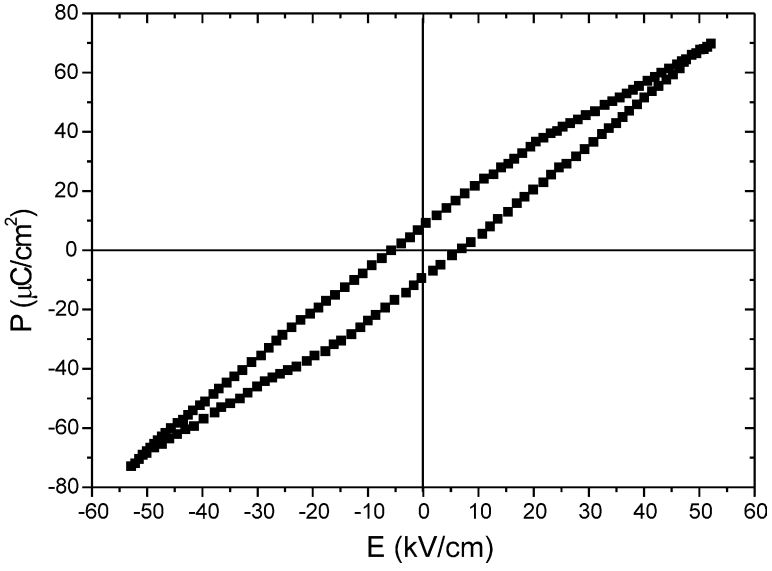

Fig. 11. Hysteresis loop of a $BiGeB_6$ glass-ceramic of 240±2 μm thickness, heated at 480 °C for 12 h.

comparable to that of $BaTiO_3$ ceramic but its coercive field, E_r, is larger. A thin film of $Bi_4Ti_3O_{12}$, grown along the c-axis gave a value of $P_s = 5.7$ μC/cm^2 [17] which is smaller than that of the Bi_2GeO_5 based glass-ceramic. However, the value of P_s measured along the *a*-axis of a $Bi_4Ti_3O_{12}$ single crystal could be as high as 50 μC/cm^2. Since there are some structural similarities between $Bi_4Ti_3O_{12}$ and Bi_2GeO_5 improved electrical properties might be obtained if the crystals in the glass-ceramic were aligned along the *a*-axis instead of the current preferred orientation perpendicular to the (311) planes.

Table 4
The comparison of T_C (Curie temperature), P_s (spontaneous polarisation) and E_r (coercive field) of Bi_2GeO_5 and some other well-known ferroelectrics

Ferroelectrics	T_C (°C)	P_s (at room temperature) ($\mu C/cm^2$)	E_r (kV/cm)
Bi_2GeO_5 (glass-ceramic)	–	14.0 ± 0.5	5.6 ± 0.2
$BaTiO_3$[16](Ceramic)	≈120	≈13	≈0.3
$Bi_4Ti_3O_{12}$[15] (*c*-axis thin film)	≈675	≈5.7	≈130

4. Conclusions

The $BiO_{1.5}$–GeO_2–$BO_{1.5}$ system was investigated to address the problem of the devitrification of stoichiometric Bi_2GeO_5 glass. Pure Bi_2GeO_5 glass-ceramic could be successfully formed from the $BiO_{1.5}$–GeO_2–$BO_{1.5}$ system. The dielectric behaviour and hysteresis loop confirmed the ferroelectric character of this Bi_2GeO_5 based glass-ceramic, having $P_s = 14.0 \pm 0.5\ \mu C/cm^2$. This value of P_s is comparable with that of $BaTiO_3$ ceramic but a high voltage was used for poling. The preferred growth direction of this glass-ceramic is perpendicular to the (311) planes of Bi_2GeO_5 but *a*-axis orientation may be preferable, in order to enhance the electrical properties. Therefore the grain-oriented glass-ceramic method should be attempted in future work.

Acknowledgements

The authors wish to thank Dr. David Hall, Dr. Jiang Quanzhong and Anuson Niyompan for their continuous assistance throughout the dielectric measurement and ferroelectric hysteresis loop and K. Pengpat would like to record her thanks to the DPST project and Thai Government for financial support.

References

1. Nitsche, R., *Journal of Applied Physics*, 1965, **36**, 2358.
2. Ballman, A. A., *Journal of Crystal Growth*, 1967, **1**, 37.
3. Abrahams, S. C., Jamieson, P. B. and Bernstein, J. L., *Journal of Chemical Physics*, 1967, **47**, 4034.
4. Levin, E. M. and Roth, R. S., *J. Res. Natl. Bur. Standards*, 1964, **68A**, 201.
5. Speranskaya, E. I. and Arshakun, A. A., *Zh. Neorgan. Khim*, 1964, **9**, 417.
6. Firsov, A. V., Skorokhodov, N. E., Astaf'ev, A. V., Stefanovich, S.Yu. and Venevtsev, Yu. N., *Kristallografiya*, 1984, **29**, 509.
7. Auriviltius, B., Lindblom, C. I. and Stenson, P., *Acta Chemica Scandinavica*, 1964, **18**, 1556.
8. Hahn, T., *International Tables for Crystallography*, Vol. A: Space-group Symmetry, D. Reidel Publishing Company, 1987.
9. Pengpat, K., 2000, *PhD thesis*, University of Warwick, UK.
10. Nassau, K. and Chadwick, D. L., *Journal of the American Ceramic Society*, 1982, **65**, 197.
11. JCPDS International Centre for Diffraction Data.
12. Sawyer, C. B. and Tower, C. H., *Phys. Rev.*, 1930, **57**, 54.
13. Glazer, A. M., Groves, P. and Smith, D. T., *J. Physics E: Sci Instruments*, 1984, **17**, 95.
14. Shelby, J. E. *Introduction to Glass Science and Technology*, The Royal Society of Chemistry, 1997.
15. Topping, J. A., Cameron, N. and Murthy, M. K., *Journal of the American Ceramic Society*, 1974, **57**, 519.
16. Borelli, N. F. and Layton, M. M., *J. Non-Cryst. Solids*, 1971, **6**, 197.
17. Wu, S. Y., *Journal of Applied Physics*, 1979, **50**, 4314.